Catalysis Science & Technology

Accepted Manuscript

ROYAL SOCIETY OF CHEMISTRY

www.rsc.org/catalysis

Catalysis Science & Technology

Catalysis Science & Technology

Dynamic Article Links ►

Cite this: DOI: 10.1039/c0xx00000x

PAPER

www.rsc.org/xxxxxx

Mechanism of the effect of H_2O on the low temperature selective catalytic reduction of NO with NH_3 over Mn-Fe spinel

Shangchao Xiong, Yong Liao, Xin Xiao, Hao Dang, Shijian Yang *

Received (in XXX, XXX) Xth XXXXXXXXX 20XX, Accepted Xth XXXXXXXXX 20XX

DOI: 10.1039/b000000x

H_2O showed a notable inhibition on the low temperature selective catalytic reduction (SCR) reaction over Mn based catalysts. However, the mechanism of H_2O effect was not clear. In this work, the mechanism of H_2O effect on the low temperature SCR reaction over Mn-Fe spinel was studied using the transient reaction study and the steady-state kinetic analysis. According to the steady-state kinetic analysis, the reaction kinetic rate constants of NO reduction over Mn-Fe spinel (including the rate constants of N_2 formation through the Eley-Rideal mechanism and the Langmuir -Hinshelwood mechanism, and the rate constants of N_2O formation) in the presence of H_2O and in the absence of H_2O were compared. According to the transient reaction study, the effect of H_2O on the elementary reactions of NO reduction over Mn-Fe spinel through both the Eley-Rideal mechanism and the Langmuir-Hinshelwood mechanism was investigated. The results indicated that the effect of H_2O on the low temperature SCR reaction over Mn-Fe spinel was not only attributed to the competition adsorption of H_2O with NH_3 and NO_x, but also related to the decrease of the oxidation ability and the inhibition of the interface reaction.

1. Introduction

Because the space and access for the operation of high temperature selective catalytic reduction (SCR) catalysts for example V_2O_5-$WO_3(MoO_3)/TiO_2$ are limited in many existing coal-fired power plants, [1] there is a strong demand for the low temperature SCR catalysts, [2] which can be placed downstream of the electrostatic precipitator and desulfurizer. So far, Mn based catalysts, for example MnO_x/TiO_2, [3-7] MnO_x-CeO_2, [8, 9] MnO_x-CeO_2/TiO_2, [10] and Fe_2O_3-MnO_2/TiO_2 [11] have been regarded as the most promising low temperature SCR catalysts. However, Mn based catalysts are currently extremely restricted in the application for at least three reasons: the lower N_2 selectivity, the unrecoverable deactivation by SO_2 and the recoverable deactivation by H_2O. [2, 12]

Mn-Fe spinel showed an excellent low temperature SCR performance, whose pseudo-first rate constant of NO reduction was close to that of MnO_x-CeO_2. [12] Meanwhile, N_2 selectivity of NO reduction over Mn-Fe spinel was much better than that over MnO_x-CeO_2. [13, 14] Furthermore, magnetic Mn-Fe spinel deactivated by SO_2 due to the deposition of $NH_4HSO_4/(NH_4)_2SO_4$ and the sulfation of catalyst can be regenerated after water washing. [12]

H_2O showed an obvious inhibition on the low temperature SCR reaction over Mn-Fe spinel, while N_2 selectivity of NO reduction over Mn-Fe spinel increased remarkably after the introduction of H_2O. [13, 14] The recoverable deactivation of Mn based catalysts by H_2O was generally attributed to the competition adsorption of H_2O with NH_3. [15, 16] However, the improvement of N_2 selectivity in the presence of H_2O cannot be explained by the competition adsorption. As in situ DRIFT spectra study is difficult to be performed in the presence of a high concentration of water vapor, the mechanism of H_2O effect on the low temperature SCR reaction over Mn-Fe spinel was investigated in this work using the steady-state kinetic study and the transient reaction study. To compare the reaction kinetic rate constants of NO reduction over Mn-Fe spinel in the absence and in the presence of H_2O, the steady-state kinetic study was performed. To study the influence of H_2O on the elementary reactions of N_2O and N_2 formation over Mn-Fe spinel through both the Eley-Rideal mechanism and the Langmuir-Hinshelwood mechanism, the transient reaction study was conducted. The results indicated that the effect of H_2O on the low temperature SCR reaction over Mn-Fe spinel was not only attributed to the competition adsorption of H_2O with NH_3 and NO_x, but also related to the decrease of the oxidation ability and the inhibition of the interface reaction.

2. Experimental

2.1 Catalyst preparation

Mn-Fe spinel was prepared using a co-precipitation method. [12, 17, 18] The solution of the mixture of ferrous sulfate, ferric chloride, and manganese sulfate (Fe^{3+}:Fe^{2+}:Mn^{2+}=4:1:1, and total cation amount=0.075 mol) was added to an ammonia solution (100 mL) with 800 rpm of stirring. The particles were then separated by

centrifugation and washed with distilled water 3 times. At last, the particles were calcined under air at 400 °C for 3 h after dried at 105 °C for 12 h.

2.2 Catalytic test

The catalytic reaction was performed on a fixed-bed quartz tube reactor. [12, 19, 20] The mass of catalyst with 40-60 mesh was 100 mg, the total flow rate was 200 mL min^{-1}, and the corresponding gas hourly space velocity (GHSV) was 120000 cm^3 g^{-1} h^{-1}. The typical reactant gas contained 500 ppm of NH_3 (when used), 500 ppm of NO (when used), 2% of O_2, 5% of H_2O (when used) and balance of N_2. The gas composition in the outlet was continually monitored by a Fourier transform infrared spectrometer (FTIR, Thermo SCIENTIFIC, ANTARIS, IGS Analyzer).

The capacities of Mn-Fe spinel for NH_3 and NO+O_2 adsorption at 150 °C were determined using NH_3-TPD and NO-TPD, respectively. NH_3-TPD and NO-TPD were carried out on the fixed-bed quartz tube reactor. Before the experiment, about 0.10 g of Mn-Fe spinel was pretreated under N_2 atmosphere (200 mL min^{-1}) at 300 °C for 60 min to remove adsorbed H_2O and other gases. After Mn-Fe spinel was cooled to 150 °C, the N_2 flow was switched to a flow of 500 ppm of NH_3 or 500 ppm of NO+2% of O_2 (200 ml min^{-1}) for 120 min. The sample was then purged by N_2 (200 ml min^{-1}) for another 30 min. NH_3-TPD and NO-TPD were performed at a heating rate of 10 °C min^{-1} to 700 °C under a N_2 flow (200 ml min^{-1}).

2.3 Steady-state kinetic study

To determine the rate constants of NO reduction over Mn-Fe spinel, the steady-state kinetic study was conducted. Gaseous NH_3 concentration in the inlet was kept at 500 ppm, while gaseous NO concentration varied from 200 to 500 ppm. [2, 13, 14] To overcome the diffusion limitation (including the inner diffusion and external diffusion), a very high GHSV of 1200000-4800000 cm^3 g^{-1} h^{-1} (the catalyst mass ranged from 5 to 20 mg, and the total flow rate was 400 mL) was adopted to obtain less than 15% of NO_x conversion.

2.4 Transient reaction study

To study the effect of H_2O on the elementary reactions of N_2O formation over Mn-Fe spinel through the Eley-Rideal mechanism, the amounts of N_2O formed during passing NO+O_2 over NH_3 presorbed Mn-Fe spinel, passing NO+O_2+H_2O over NH_3 presorbed Mn-Fe spinel, and passing NO+O_2 over NH_3+H_2O presorbed Mn-Fe spinel and passing NO+O_2+H_2O over NH_3+H_2O presorbed Mn-Fe spinel were compared. To study the effect of H_2O on the elementary reactions of N_2O formation over Mn-Fe spinel through the Langmuir-Hinshelwood mechanism, the amounts of N_2O formed during passing NH_3 over NO+O_2 presorbed Mn-Fe spinel, passing NH_3+H_2O over NO+O_2 presorbed Mn-Fe spinel, and passing NH_3 over NO+O_2+H_2O presorbed Mn-Fe spinel and passing NH_3+H_2O over NO+O_2+H_2O presorbed Mn-Fe spinel were compared.

3. Results

3.1 Effect of H_2O on the SCR reaction over Mn-Fe spinel

As shown in Fig. 1, Mn-Fe spinel showed an excellent SCR activity at low temperatures, and NO_x conversion was higher than 80% above 140 °C with the GHSV of 1200000 cm^3 g^{-1} h^{-1}. Furthermore, a lot of N_2O formed during the SCR reaction over Mn-Fe spinel, and N_2O selectivity obviously increased with the increase of reaction temperature from 120 to 200 °C. Fig. 1 shows that NO_x conversion over Mn-Fe spinel obviously decreased as 5% of H_2O added. Meanwhile, N_2O selectivity of NO reduction over Mn-Fe spinel in the presence of 5% of H_2O was much less than that in the absence of H_2O. They suggest that NO reduction and N_2O formation over Mn-Fe spinel were both restrained in the presence of H_2O. This result was consistent with the result of our previous study on Mn-Fe spinel. [12, 14]

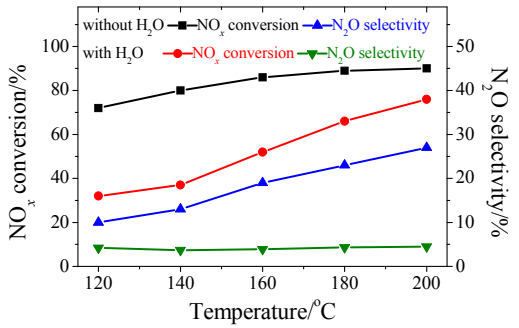

Fig. 1 Effect of 5% of H_2O on the SCR performance of Mn-Fe spinel. Reaction conditions: [NH_3]=[NO]=500 ppm, [O_2]=2%, catalyst mass=100 mg, total flow rate=200 mL min^{-1} and GHSV=120000 cm^3 g^{-1} h^{-1}.

3.2 Effect of H_2O on NO and NH_3 adsorption on Mn-Fe spinel

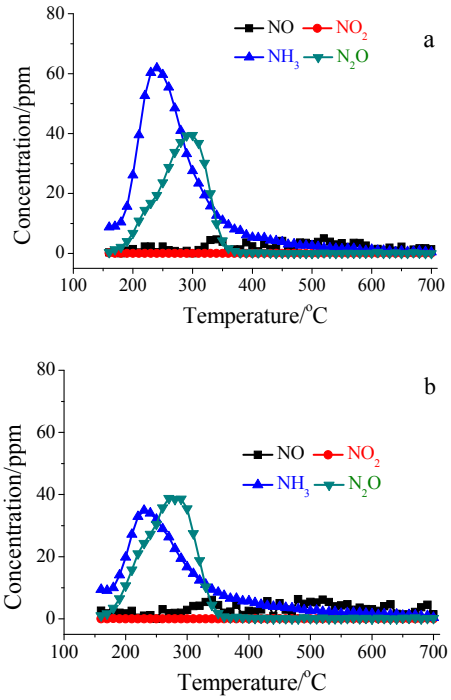

Fig. 2 NH_3-TPD profiles of Mn-Fe spinel: (a), saturated with NH_3 adsorption in the absence of H_2O at 150 °C; (b), saturated with NH_3 adsorption in the presence of 5% of H_2O at 150 °C.

The inhibition of NO reduction over Mn based catalysts by H_2O was generally attributed to the competition adsorption of H_2O with NH_3 and NO_x. [15, 16] Therefore, the effect of 5% of H_2O

on the adsorption of NH_3 and NO_x on Mn-Fe spinel was studied. Fig. 2 shows the NH_3-TPD profiles of Mn-Fe spinel saturated with NH_3 adsorption at 150 °C in the absence of H_2O and in the presence of 5% of H_2O. The capacities of Mn-Fe spinel for NH_3 adsorption at 150 °C in the absence of H_2O and that in the presence of 5% of H_2O, which were calculated from the NH_3-TPD profiles, are listed in Table 1. Table 1 shows that the capacity of Mn-Fe spinel for NH_3 adsorption in the presence of 5% of H_2O was less than that in the absence of H_2O. It suggests that the adsorption of NH_3 on Mn-Fe spinel was restrained by H_2O due to the competition adsorption, which was also supported by Fig. 3a. The breakthrough curves of NH_3 adsorbed on fresh Mn-Fe spinel and it pretreated by 5% of H_2O (Fig. 3a) show that the pretreatment of Mn-Fe spinel by H_2O showed an obvious inhibition on the adsorption of NH_3.

Table 1 Capacity of Mn-Fe spinel for NH_3 and NO_x adsorption at 150 °C /μmol g^{-1}

	NH_3	NO_x
in the absence of H_2O	122	82
in the presence of 5% of H_2O	105	46

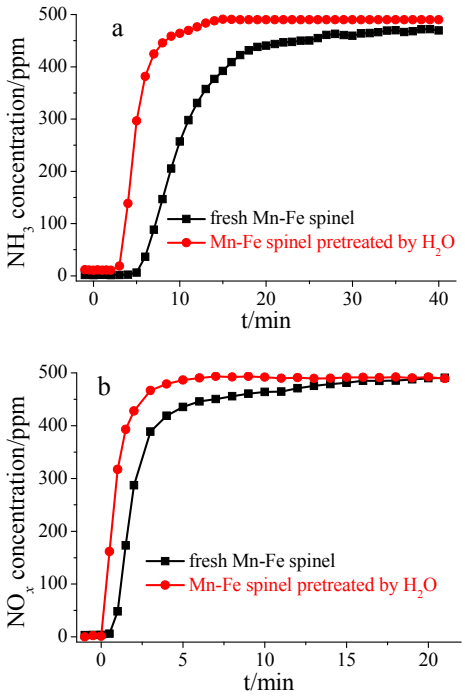

Fig. 3 Effect of the pretreatment of Mn-Fe spinel by H_2O on the adsorption of (a) NH_3 and (b) NO+O_2 at 150 °C.

Fig. 4 shows the NO_x-TPD profiles of Mn-Fe spinel saturated with NO+O_2 adsorption at 150 °C in the absence of H_2O and in the presence of 5% of H_2O. The capacities of Mn-Fe spinel for NO+O_2 adsorption at 150 °C in the absence of H_2O and that in the presence of 5% of H_2O, which were calculated from the NO_x-TPD profiles, are listed in Table 1. Table 1 shows that the capacity of Mn-Fe spinel for NO+O_2 adsorption at 150 °C in the presence of 5% of H_2O was much less than that in the absence of H_2O. It suggests that the adsorption of NO+O_2 on Mn-Fe spinel was obviously restrained by H_2O. This result was consistent with the breakthrough curves of NO+O_2 adsorbed on fresh Mn-Fe spinel and it pretreated by 5% of H_2O (Fig. 3b). The desorbed NO_x species from Mn-Fe spinel saturated with NO+O_2 adsorption in the absence of H_2O was mainly NO_2 (shown in Fig. 4a), while it from the adsorption in the presence of 5% H_2O was mainly NO (shown in Fig. 4b). There is generally agreement that the desorbed NO and NO_2 resulted from the decomposition of nitrite and nitrate, respectively. [21-25] It suggests that the further oxidization of NO_2^- to NO_3^- on Mn-Fe spinel was suppressed by H_2O. [14]

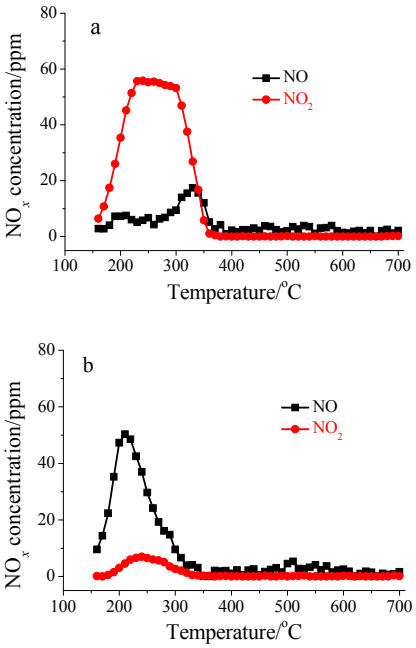

Fig. 4 NO-TPD profiles of Mn-Fe spinel: (a), saturated with the adsorption of NO+O_2 in the absence of H_2O at 150 °C; (b), saturated with the adsorption of NO+O_2 in the presence of H_2O at 150 °C.

3.3 Effect of H_2O on NO and NH_3 oxidation over Mn-Fe spinel

Table 2 Effect of 5% of H_2O on NH_3 oxidation over Mn-Fe spinel /%

	Temperature/ °C	NH_3 conversion	Selectivity		
			N_2	N_2O	NO_x
in the absence of H_2O	120	10	88	12	0
	140	19	86	14	0
	160	33	83	17	0
	180	53	80	20	0
	200	75	74	26	0
in the presence of 5% of H_2O	120	3.5	99	1	0
	140	3.7	99	1	0
	160	4	99	1	0
	180	4.5	98	2	0
	200	6.5	96	4	0

Reaction conditions: [NH_3]=500 ppm, [O_2]=2%, catalyst mass=100 mg, total flow rate=200 mL min^{-1} and GHSV=120000 cm^3 g^{-1} h^{-1}.

Table 2 and Fig. 5 show the effect of H_2O on NH_3 and NO oxidation over Mn-Fe spinel. Mn-Fe spinel showed an excellent activity for NH_3 oxidation, and NH_3 conversion was higher than 50% above 180 °C with the GHSV of 1200000 cm^3 g^{-1} h^{-1}. Meanwhile, some N_2O formed during NH_3 oxidation. However, the amount of N_2O formed from the catalytic oxidation of NH_3 was much less than that formed during the SCR reaction over Mn-Fe spinel. Meanwhile, NH_3 conversion was close to NO conversion during the SCR reaction over Mn-Fe spinel (the data

were not shown). It suggests that the catalytic oxidation of NH_3 can be approximately neglected during the SCR reaction over Mn-Fe spinel and N_2O formed during the SCR reaction over Mn-Fe spinel mainly resulted from the non selective catalytic reduction (NSCR) reaction. Table 2 also shows that the oxidation of NH_3 was completely suppressed in the presence of 5% of H_2O (shown in Table 2). Meanwhile, the oxidation of NO to NO_2 was obviously restrained in the presence of H_2O (shown in Fig. 5). The catalytic oxidation of NO and NH_3 over Mn-Fe spinel was mainly related to the amounts of NH_3 and NO_x adsorbed on Mn-Fe spinel and the oxidation ability of Mn-Fe spinel. [26-28] In comparison of Table 2 and Fig. 5 with Table 1, the inhibition on NH_3 oxidation and NO oxidation by H_2O was much remarkable than that on NH_3 adsorption and NO+O_2 adsorption. It suggests that the oxidation ability of Mn-Fe spinel obviously decreased in the presence of H_2O.

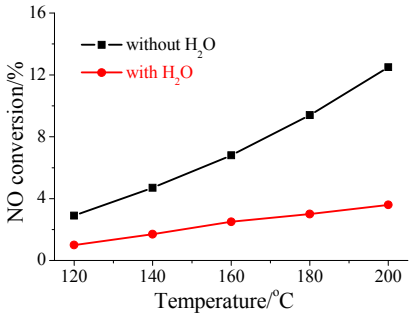

Fig. 5 Effect of 5% of H_2O on NO oxidation over Mn-Fe spinel. Reaction conditions: [NO]=500 ppm, [O_2]=2%, catalyst mass=100 mg, total flow rate=200 mL min^{-1} and GHSV=120000 cm^3 g^{-1} h^{-1}.

4. Discussion

4.1 Reaction mechanism

According to the transient reaction study and in situ DRIFT spectra study (shown in the Supporting Information), our previous studies demonstrated that both the Langmuir-Hinshelwood mechanism (i.e. the reaction between adsorbed NO_x species and adsorbed NH_3 species) and the Eley-Rideal mechanism (i.e. the reaction between adsorbed NH_3 species and gaseous NO) contributed to NO reduction (including N_2 formation and N_2O formation) over Mn-Fe spinel. [12, 14] NO reduction over Mn-Fe spinel through the Langmuir-Hinshelwood mechanism can be approximately described as: [12, 14, 29]

$$NH_{3(g)} \rightarrow NH_{3(ad)} \quad (1)$$

$$NO_{(g)} \rightarrow NO_{(ad)} \quad (2)$$

$$\equiv Mn^{4+}{=}O + NO_{(ad)} \rightarrow \equiv Mn^{3+}\text{-O-NO} \quad (3)$$

$$\equiv Mn^{3+}\text{-O-NO} + \frac{1}{2}O_2 \rightarrow \equiv Mn^{3+}\text{-O-}NO_2 \quad (4)$$

$$\equiv Mn^{3+}\text{-O-NO+}NH_{3(ad)} \rightarrow \equiv Mn^{3+}\text{-O-NO-}NH_3 \rightarrow \equiv Mn^{3+}\text{-OH+}N_2\text{+}H_2O \quad (5)$$

$$\equiv Mn^{3+}\text{-O-}NO_2 + NH_{3(ad)} \rightarrow \equiv Mn^{3+}\text{-O-}NO_2\text{-}NH_3 \rightarrow \equiv Mn^{3+}\text{-OH+}N_2O + H_2O \quad (6)$$

$$\equiv Mn^{3+}\text{-OH} + \frac{1}{4}O_2 \rightarrow \equiv Mn^{4+}{=}O + \frac{1}{2}H_2O \quad (7)$$

The SCR reaction over Mn-Fe spinel started with the adsorption of NH_3 (i.e. Reaction 1). Meanwhile, gaseous NO can be physically adsorbed on Mn-Fe spinel, [22] which was then oxidized by Mn^{4+} on the surface to form monodentate NO_2^- (i.e. Reaction 3). Besides to be further oxidized to monodentate NO_3^- (i.e. Reaction 4), [21] adsorbed NO_2^- can react with adsorbed NH_3 on the adjacent sites to form NH_4NO_2 (i.e. Reaction 5), which was then decomposed to N_2 and H_2O. Adsorbed monodentate NO_3^- can react with adsorbed NH_3 species on the adjacent sites to form NH_4NO_3 (i.e. Reaction 6), which was then decomposed to N_2O. [22] Reaction 7 was the regeneration of Mn^{4+} on the surface.

Meanwhile, NO reduction over Mn-Fe spinel through the Eley-Rideal mechanism can be approximately described as: [12, 14, 22, 29]

$$NH_{3(g)} \rightarrow NH_{3(ad)} \quad (1)$$

$$NH_{3(ad)} + \equiv Mn^{4+}{=}O \rightarrow NH_2 + \equiv Mn^{3+}\text{-OH} \quad (8)$$

$$NH_2 + NO_{(g)} \rightarrow N_2 + H_2O \quad (9)$$

$$NH_2 + \equiv Mn^{4+}{=}O \rightarrow NH + \equiv Mn^{3+}\text{-OH} \quad (10)$$

$$NH + NO_{(g)} + Mn^{4+}{=}O \rightarrow N_2O + Mn^{3+}\text{-OH} \quad (11)$$

$$\equiv Mn^{3+}\text{-OH} + \frac{1}{4}O_2 \rightarrow \equiv Mn^{4+}{=}O + \frac{1}{2}H_2O \quad (7)$$

Reaction 8 was the activation of adsorbed NH_3 by Mn^{4+} on Mn-Fe spinel to form NH_2, which then reacted with gaseous NO to form N_2 (i.e. Reaction 9). Meanwhile, NH_2 on Mn-Fe spinel can be further oxidized to NH (i.e. Reaction 10), which then reacted with gaseous NO to form N_2O (i.e. Reaction 11).

The kinetic equations of N_2O and N_2 formation through the Langmuir-Hinshelwood mechanism (i.e. Reactions 5 and 6) can be described as:

$$\frac{d[N_2O]}{dt}\Big|_{L\text{-}H} = k_1[Mn^{3+}\text{-O-}NO_2\text{-}NH_3] \quad (12)$$

$$\frac{d[N_2]}{dt}\Big|_{L\text{-}H} = k_2[Mn^{3+}\text{-O-NO-}NH_3] \quad (13)$$

Where, k_1, k_2, [Mn^{3+}-O-NO_2-NH_3] and [Mn^{3+}-O-NO-NH_3] were the rate constants of NH_4NO_3 and NH_4NO_2 decomposition and the concentrations of NH_4NO_3 and NH_4NO_2 on Mn-Fe spinel, respectively.

Our previous studies demonstrated that [Mn^{3+}-O-NO-NH_3] and [Mn^{3+}-O-NO_2-NH_3] can be approximately regarded as the constants at the steady state, [14, 29] which were independent of the concentrations of gaseous NO and NH_3. Hinted by Equations 12 and 13, N_2O formation and N_2 formation through the Langmuir-Hinshelwood mechanism were both not related to gaseous NO and NH_3 concentrations, and the reaction orders of N_2 and N_2O

formation through the Langmuir-Hinshelwood mechanism with respect to gaseous NO concentration were both nearly zero.

The kinetic equations of N_2O and N_2 formation through the Eley-Rideal mechanism (i.e. Reactions 9 and 11) can be described as: [13]

$$\left.\frac{d[N_2O]}{dt}\right|_{E\text{-}R} = -\frac{d[NH]}{dt} = k_3[NH][NO_{(g)}][Mn^{4+}{=}O] \quad (14)$$

$$\left.\frac{d[N_2]}{dt}\right|_{E\text{-}R} = -\frac{d[NH_2]}{dt} = k_4[NH_2][NO_{(g)}] \quad (15)$$

Where, k_3, k_4, $[NO_{(g)}]$, $[NH_2]$, $[NH]$ and $[Mn^{4+}{=}O]$ were the rate constants of Reactions 11 and 9, gaseous NO concentration and the concentrations of NH_2, NH and Mn^{4+} on Mn-Fe spinel, respectively.

The kinetic equations of NH_2 and NH formation on Mn-Fe spinel (i.e. Reactions 8 and 10) can be described as:

$$\frac{d[NH_2]}{dt} = k_5[NH_{3(ad)}][Mn^{4+}{=}O] \quad (16)$$

$$\frac{d[NH]}{dt} = -\frac{d[NH_2]}{dt} = k_6[NH_2][Mn^{4+}{=}O] \quad (17)$$

Where, $[NH_{3(ad)}]$, k_5 and k_6 were the concentration of NH_3 adsorbed, the reaction rate constants of Reactions 8 and Reaction 10, respectively.

According to Equations 15-17, the variation of NH_2 on Mn-Fe spinel can be described as:

$$\begin{aligned} -\frac{d[NH_2]}{dt} &= k_6[NH_2][Mn^{4+}{=}O] \\ &+k_4[NH_2][NO_{(g)}] - k_5[NH_{3(ad)}][Mn^{4+}{=}O] \end{aligned} \quad (18)$$

NH_2 concentration on Mn-Fe spinel would not change at the steady state. Therefore,

$$\frac{d[NH_2]}{dt} = 0 \quad (19)$$

Thus,

$$[NH_2] = \frac{k_5[NH_{3(ad)}][Mn^{4+}{=}O]}{k_6[Mn^{4+}{=}O] + k_4[NO_{(g)}]} \quad (20)$$

Then, the kinetic equation of N_2 formation through the Eley-Rideal mechanism (i.e. Equation 15) would be transformed as:

$$\begin{aligned} \left.\frac{d[N_2]}{dt}\right|_{E\text{-}R} &= k_4[NH_2][NO_{(g)}] \\ &= k_4[NO_{(g)}]\frac{k_5[NH_{3(ad)}][Mn^{4+}{=}O]}{k_6[Mn^{4+}{=}O] + k_4[NO_{(g)}]} \end{aligned} \quad (21)$$

If the rate of N_2O formation was very low (for example the SCR reaction over Mn-Fe spinel in the presence of 5% of H_2O), the value of $k_6[Mn^{4+}{=}O][NH_2]$ would be close to zero (hinted by Equation 17). Therefore, N_2 formation through the Eley-Rideal mechanism would be approximately independent of gaseous NO concentration. Meanwhile, Equation 13 shows that N_2 formation through the Langmuir-Hinshelwood mechanism was not related to gaseous NO concentration. They suggest that the reaction order of N_2 formation over Mn-Fe spinel with respect to gaseous NO concentration would be nearly zero. However, Fig. 6 shows that the rate of N_2 formation remarkably increased with the increase of gaseous NO concentration in the presence of H_2O. They indicate the rate of NH_2 formation (i.e. Equation 16) was much higher than the rate of NH_2 reduction (i.e. Equations 15 and 17) and NH_2 reduced through Reactions 9 and 10 can be rapidly recovered through Reaction 8. Therefore, NH_2 concentration on Mn-Fe spinel at the steady state can be approximately regarded as a constant,[13, 14] which was not related to the concentrations of gaseous NO and gaseous NH_3. Hinted by Equation 16, NH_2 concentration on Mn-Fe spinel depended on the oxidation ability of Mn-Fe spinel, and the concentrations of NH_3 adsorbed and Mn^{4+} on Mn-Fe spinel.

NH on Mn-Fe spinel resulted from the further oxidation of NH_2 (i.e. Reaction 10), and it was consumed through Reaction 11. NH concentration on Mn-Fe spinel would not change at the steady state. Therefore,

$$\begin{aligned} \frac{d[NH]}{dt} &= k_6[NH_2][Mn^{4+}{=}O] \\ &-k_3[NH][NO_{(g)}][Mn^{4+}{=}O] = 0 \end{aligned} \quad (22)$$

Thus,

$$[NH] = \frac{k_6[NH_2]}{k_3[NO_{(g)}]} \quad (23)$$

Then, the kinetic equation of N_2O formation over Mn-Fe spinel through the Eley-Rideal mechanism (i.e. Equation 14) can be transformed as:

$$\begin{aligned} \left.\frac{d[N_2O]}{dt}\right|_{E\text{-}R} &= k_3[NH][NO_{(g)}][Mn^{4+}{=}O] \\ &= k_3\frac{k_6[NH_2]}{k_3[NO_{(g)}]}[NO_{(g)}][Mn^{4+}{=}O] \\ &= k_6[NH_2][Mn^{4+}{=}O] \end{aligned} \quad (24)$$

According to Equations 12, 13, 15 and 24, the kinetic equations of NO reduction and N_2O formation over Mn-Fe spinel can be described as follows:

$$\begin{aligned} \frac{d[N_2O]}{dt} &= \left.\frac{d[N_2O]}{dt}\right|_{E\text{-}R} + \left.\frac{d[N_2O]}{dt}\right|_{L\text{-}H} \\ &= k_6[NH_2][Mn^{4+}{=}O] + k_1[Mn^{3+}\text{-}O\text{-}NO_2\text{-}NH_3] \\ &= k_{N_2O} \end{aligned} \quad (25)$$

$$\begin{aligned} -\frac{d[NO_{(g)}]}{dt} &= \left.\frac{d[N_2]}{dt}\right|_{E\text{-}R} + \left.\frac{d[N_2]}{dt}\right|_{L\text{-}H} + \frac{d[N_2O]}{dt} \\ &= k_4[NH_2][NO_{(g)}] + k_2[Mn^{3+}\text{-}O\text{-}NO\text{-}NH_3] \\ &+ k_6[NH_2][Mn^{4+}{=}O] + k_1[Mn^{3+}\text{-}O\text{-}NO_2\text{-}NH_3] \\ &= k_{N_2(E\text{-}R)}[NO_{(g)}] + k_{N_2(L\text{-}H)} + k_{N_2O} \end{aligned} \quad (26)$$

Where, $k_{N2(E\text{-}R)}$, $k_{N2(L\text{-}H)}$ and k_{N2O} were the reaction rate constants of N_2 formation over Mn-Fe spinel through the Eley-

Rideal mechanism, that of N_2 formation through the Langmuir-Hinshelwood mechanism and that of N_2O formation. $k_{N2(E-R)}$, $k_{N2(L-H)}$ and $k_{N2(E-R)}$ can be described as:

$$k_{N_2(E\text{-}R)} = k_4[NH_2] \quad (27)$$

$$k_{N_2(L\text{-}H)} = k_2[Mn^{3+}\text{-}O\text{-}NO\text{-}NH_3] \quad (28)$$

$$k_{N_2O} = k_6[NH_2][Mn^{4+}{=}O] + k_1[Mn^{3+}\text{-}O\text{-}NO_2\text{-}NH_3] \quad (29)$$

4.2 Steady-state kinetic study

To obtain the rate constants of NO reduction over Mn-Fe spinel (i.e. $k_{N2(E-R)}$, $k_{N2(L-H)}$ and k_{N2O}), the steady-state kinetic study was performed. [2] Figs. 6a and 6b show that there was an excellent linear relationship between the rate of NO reduction and gaseous NO concentration, which was consistent with the hint of Equation 26. [14] Meanwhile, Figs. 6c and 6d show that the rate of N_2O formation was generally independent of gaseous NO concentration, which was consistent with the hint of Equation 25. [14] Therefore, the rate constants of NO reduction over Mn-Fe spinel (i.e. $k_{N2(E-R)}$, $k_{N2(L-H)}$ and k_{N2O}) in the presence and in the absence of H_2O can be calculated from Fig. 6 after the linear regression, which are listed in Table 3.

Table 3 shows that $k_{N2(E-R)}$ and k_{N2O} of NO reduction over Mn-Fe spinel in the presence of H_2O were both much less than those in the absence of H_2O. They suggest that N_2 formation through Eley-Rideal mechanism and N_2O formation over Mn-Fe spinel were both restrained remarkably by H_2O. Furthermore, Table 3 also shows that the decrease of k_{N2O} due to the presence of H_2O was much faster than the decrease of $k_{N2(E-R)}$. It suggests that the inhibition of N_2O formation over Mn-Fe spinel by H_2O was much more remarkable than the inhibition on N_2 formation, resulting in an obvious decrease of N_2O selectivity (shown in Fig. 1).

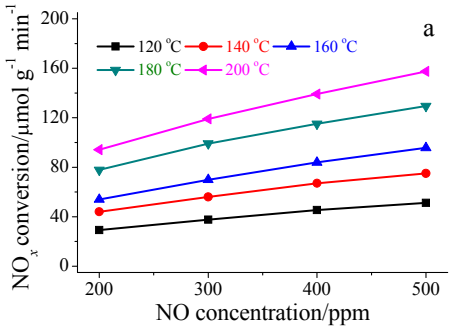

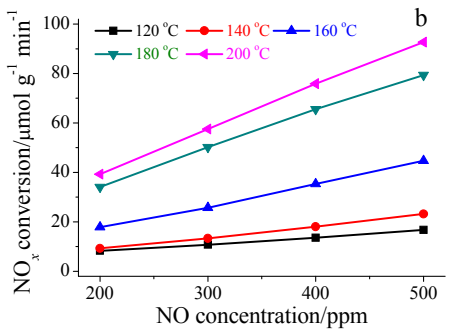

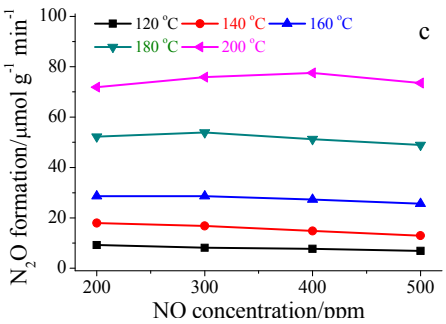

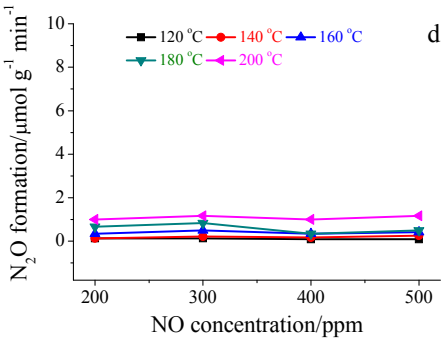

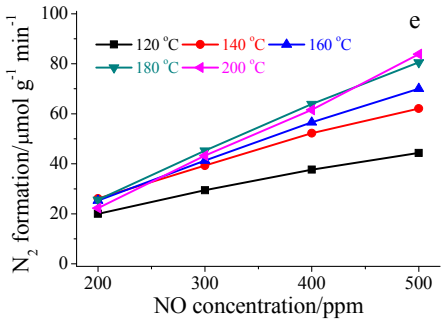

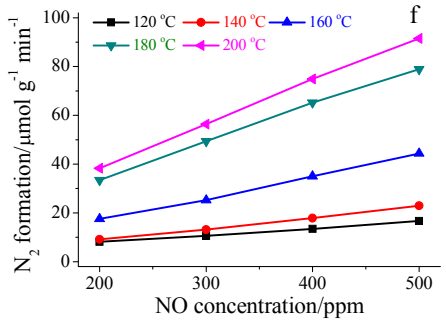

Fig. 6 Dependence of NO conversion rate on gaseous NO concentration during the SCR reaction over Mn-Fe spinel: (a), in the absence of H_2O; (b), in the presence of 5% of H_2O; Dependence of N_2O formation rate on gaseous NO concentration during the SCR reaction over Mn-Fe spinel: (c), in the absence of H_2O; (d), in the presence of 5% of H_2O;Dependence of N_2 formation rate on gaseous NO concentration during the SCR reaction over Mn-Fe spinel: (e), in the absence of H_2O; (f), in the presence of 5% of H_2O. Reaction conditions: $[NH_3]$=500 ppm, [NO]=200-500 ppm, $[O_2]$=2%, catalyst mass=5-20 mg, total flow rate=400 mL min^{-1} and GHSV=1200000-4800000 cm^3 g^{-1} h^{-1}.

Table 3 The rate constants of N_2 formation over Mn-Fe spinel through the Eley-Rideal mechanism ($k_{N2(E-R)}$) and the Langmuir-Hinshelwood mechanism ($k_{N2(L-H)}$), and the rate constant of N_2O formation (k_{N2O})

Temperature/°C	$-\frac{d[NO_{(g)}]^*}{dt}=k_{N_2(E-R)}[NO_{(g)}]+k_{N_2(L-H)}+k_{N_2O}$				R^2
	$k_{N2(L-H)}$ /μmol g^{-1} min^{-1}	$k_{N2(E-R)}$ /mol g^{-1} min^{-1}	k_{N2O} /μmol g^{-1} min^{-1}		
in the absence of H_2O	120	4	0.081	8	0.994
	140	3	0.12	16	0.996
	160	0	0.15	27	0.998
	180	0	0.18	51	0.999
	200	0	0.20	73	0.999
in the presence of 5% of H_2O	120	2.4	0.028	0.1	0.997
	140	0	0.047	0.2	0.997
	160	0	0.090	0.4	0.998
	180	3.9	0.15	0.5	0.999
	200	2.8	0.18	1.1	0.999

* The unit of $[NO_{(g)}]$ in this equation was m^3 m^{-3}.

4.3 Transient reaction study

To clarify the mechanism of H_2O inhibition on NO reduction over Mn-Fe spinel, the transient reaction study was conducted (shown in Figs. 7 and 8). Because N_2 formed cannot be determined in this work, N_2O was selected as a probe to study the effect of H_2O on NO reduction over Mn-Fe spinel.

After $NO+O_2$ passed over NH_3 presorbed Mn-Fe spinel, 2.3 μmol of N_2O formed (shown in Fgiure 7a). The formed N_2O mainly resulted from the Eley-Rideal mechanism.[13, 14, 29] However, only 1.5 μmol of N_2O formed during passing $NO+O_2+H_2O$ over NH_3 presorbed Mn-Fe spinel (shown in Fig. 7b). As NH_3 adsorption and the activation of adsorbed NH_3 (i.e. Reactions 1, 8 and 10) were not affected by H_2O, it suggests that k_3 in the presence of H_2O was less than that in the absence of H_2O, resulting in the inhibition of Reaction 11 by H_2O. Fig. 7c shows that approximately 1.2 μmol of N_2O formed as $NO+O_2$ passed over NH_3+H_2O presorbed Mn-Fe spinel. As the interface reaction (i.e. Reaction 11) was not affected by H_2O, it suggests that the concentration of NH on Mn-Fe spinel in the presence of H_2O was only approximately 52% of that in the absence of H_2O. NH_3-TPD profiles show that the concentration of NH_3 adsorbed on Mn-Fe spinel (i.e. $[NH_{3(ad)}]$) decreased approximately 14% in the presence of H_2O (shown in Table 1). It suggests that k_6 in the presence of H_2O was much less than that in the absence of H_2O, resulting in the inhibition of the over-activation of adsorbed NH_3 (Reaction 10). The decrease of k_6 was related to the decrease of the oxidation ability of Mn-Fe spinel in the presence of H_2O, which was hinted by the results of NH_3 oxidation and NO oxidation (shown in Fig. 5). As a result, the formation of N_2O over Mn-Fe spinel through the Eley-Rideal mechanism was obviously restrained in the presence of H_2O and only 0.9 μmol of N_2O formed during passing $NO+O_2+H_2O$ over NH_3+H_2O presorbed Mn-Fe spinel (shown in Fig. 7d). The mechanism of N_2 formation over Mn-Fe spinel through the Eley-Rideal mechanism was similar to that of N_2O formation. The decrease of the oxidation ability in the presence of H_2O also caused to the decrease of k_5. Meanwhile, the concentration of NH_3 adsorbed on Mn-Fe spinel decreased in the presence of H_2O (shown in Table 1). Hinted by Equation 16, $[NH_2]$ on Mn-Fe spinel notably decreased in the presence of H_2O. Furthermore, the decrease of k_3 in the presence of H_2O also indicates the decrease of k_4. Hinted by Equation 27, $k_{N2(E-R)}$ would decrease remarkably in the presence of H_2O, which was demonstrated in Table 3.

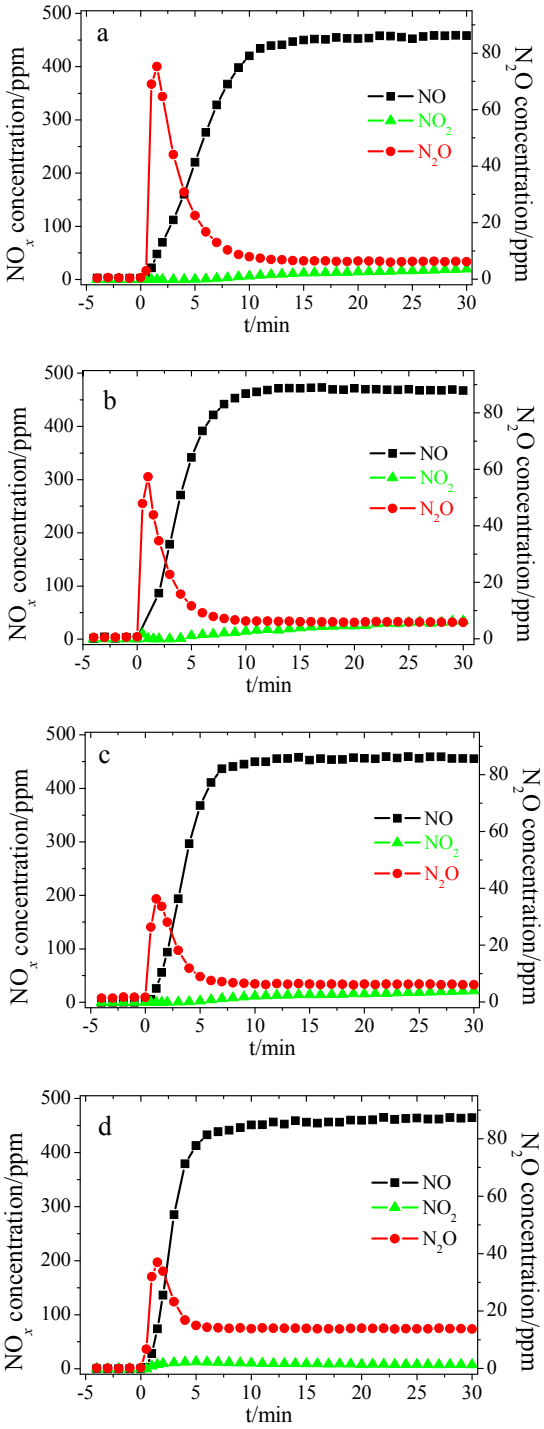

Fig. 7 Transient reaction taken at 150 °C upon: (a), passing $NO+O_2$ over NH_3 presorbed Mn-Fe spinel; (b), passing $NO+O_2+H_2O$ over NH_3 presorbed Mn-Fe spinel; (c), passing $NO+O_2$ over NH_3+H_2O presorbed Mn-Fe spinel; (d), passing $NO+O_2+H_2O$ over NH_3+H_2O presorbed Mn-Fe spinel.

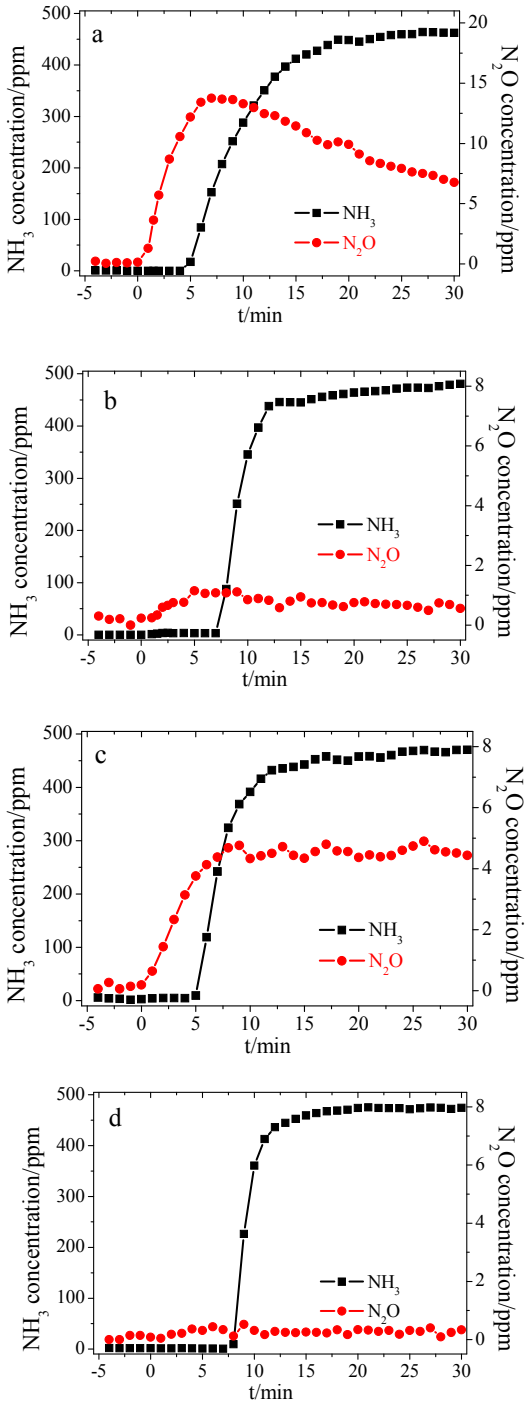

Fig. 8 Transient reaction taken at 150 ºC upon: (a), passing NH_3 over $NO+O_2$ presorbed Mn-Fe spinel; (b), passing NH_3+H_2O over $NO+O_2$ presorbed Mn-Fe spinel; (c), passing NH_3 over $NO+O_2+H_2O$ presorbed Mn-Fe spinel; (d), passing NH_3+H_2O over $NO+O_2+H_2O$ presorbed Mn-Fe spinel.

After NH_3 passed over $NO+O_2$ presorbed Mn-Fe spinel, 1.3 μmol of N_2O formed (shown in Fig. 8a). The formed N_2O mainly resulted from the Langmuir-Hinshelwood mechanism. However, only 0.1 μmol of N_2O formed during passing NH_3+H_2O over $NO+O_2$ presorbed Mn-Fe spinel (shown in Fig. 8b). As the adsorption of NO_x species on Mn-Fe spinel (i.e. Reactions 2-4) was not affected by H_2O, it suggests the formation of NH_4NO_3 and/or the decomposition of NH_4NO_3 (i.e. Reaction 6) were suppressed by H_2O. Fig. 8c shows that approximately 0.45 μmol of N_2O formed as NH_3 passed over $NO+O_2+H_2O$ presorbed Mn-Fe spinel. As the formation of NH_4NO_3 and the decomposition of NH_4NO_3 (i.e. Reaction 6) were not affected by H_2O, it suggests that the formation of NO_3^- on Mn-Fe spinel was restrained by H_2O. This result was consistent with the result of NO-TPD (shown in Fig. 4). As a result, N_2O formation over Mn-Fe spinel through the Langmuir-Hinshelwood mechanism was suppressed by H_2O and little N_2O can be observed during passing NH_3+H_2O over $NO+O_2+H_2O$ presorbed Mn-Fe spinel (shown in Fig. 8d). Therefore, the value of $k_1[Mn^{3+}\text{-}O\text{-}NO_2\text{-}NH_3]$ decreased to 0 in the presence of H_2O. Meanwhile, k_6 and $[NH_2]$ both obviously decreased in the presence of H_2O. Hinted by Equation 29, k_{N2O} in the presence of H_2O was much less than that in the absence of H_2O, which was demonstrated in Table 2.

5. Conclusion

H_2O showed a notable inhibition on NO reduction and N_2O formation over Mn-Fe spinel. NO reduction and N_2O formation over Mn-Fe spinel through the Eley-Rideal mechanism were notably restrained by H_2O due to the decrease of the oxidation ability, the inhibition of NH_3 adsorption and the inhibition of the interface reaction. Furthermore, N_2O formation over Mn-Fe spinel through the Langmuir-Hinshelwood mechanism was completely suppressed by H_2O due to the suppression of the formation and/or decomposition of NH_4NO_3.

Acknowledgements:

This study was financially supported by the National Natural Science Fund of China (Grant No. 21207067 and 41372044), the Fundamental Research Funds for the central Universities (Grant No. 30920130111023), and the Zijin Intelligent Program, Nanjing University of Science and Technology (Grant No. 2013-0106).

Notes and references

School of Environmental and biological Engineering, Nanjing University of Science and technology, Nanjing, 210094 P. R. China; E-mail: yangshijiangsq@163.com

1. Y. Liu, T. T. Gu, X. L. Weng, Y. Wang, Z. B. Wu and H. Q. Wang, J. Phys. Chem. C, 2012, 116, 16582-16592.
2. G. S. Qi and R. T. Yang, J. Catal., 2003, 217, 434-441.
3. P. G. Smirniotis, P. M. Sreekanth, D. A. Pena and R. G. Jenkins, Ind. Eng. Chem. Res., 2006, 45, 6436-6443.
4. Z. B. Wu, B. Q. Jiang, Y. Liu, H. Q. Wang and R. B. Jin, Environ. Sci. Technol., 2007, 41, 5812-5817.
5. B. Q. Jiang, Y. Liu and Z. B. Wu, J. Hazard. Mater., 2009, 162, 1249-1254.
6. Y. J. Kim, H. J. Kwon, I. S. Nam, J. W. Choung, J. K. Kil, H. J. Kim, M. S. Cha and G. K. Yeo, Catal. Today, 2011, 151, 244-250.
7. S. M. Lee, K. H. Park, S. S. Kim, D. Kwon and S. C. Hong, J. Air Waste Manage. Assoc., 2012, 62, 1085-1092.
8. G. S. Qi, R. T. Yang and R. Chang, Appl. Catal. B-environ, 2004, 51, 93-106.
9. G. S. Qi and R. T. Yang, J. Phys. Chem. B, 2004, 108, 15738-15747.
10. Z. B. Wu, R. B. Jin, Y. Liu and H. Q. Wang, Catal. Commun., 2008, 9, 2217-2220.
11. G. S. Qi and R. T. Yang, Appl. Catal. B-environ, 2003, 44, 217-225.

12. S. Yang, C. Wang, J. Li, N. Yan, L. Ma and H. Chang, Appl. Catal. B-environ, 2011, 110, 71-80.
13. S. Yang, Y. Liao, S. Xiong, F. Qi, H. Dang, X. Xiao and J. Li, J. Phys. Chem. C, 2014, 118, 21500-21508.
14. S. Yang, S. Xiong, Y. Liao, X. Xiao, F. Qi, Y. Peng, Y. Fu, W. Shan and J. Li, Environ. Sci. Technol., 2014, 48, 10354-10362.
15. Z. G. Lei, B. Han, K. Yang and B. H. Chen, Chem. Eng. J., 2013, 215, 651-657.
16. S. W. Pan, H. C. Luo, L. Li, Z. L. Wei and B. C. Huang, J. Mol. Catal. A-chem, 2013, 377, 154-161.
17. S. J. Yang, Y. F. Guo, N. Q. Yan, D. Q. Wu, H. P. He, Z. Qu and J. P. Jia, Ind. Eng. Chem. Res., 2011, 50, 9650-9656.
18. S. Yang, N. Yan, Y. Guo, D. Wu, H. He, Z. Qu, J. Li, Q. Zhou and J. Jia, Environ. Sci. Technol., 2011, 45, 1540-1546.
19. S. J. Yang, Y. F. Guo, H. Z. Chang, L. Ma, Y. Peng, Z. Qu, N. Q. Yan, C. Z. Wang and J. H. Li, Appl. Catal. B-environ, 2013, 136, 19-28.
20. S. J. Yang, J. H. Li, C. Z. Wang, J. H. Chen, L. Ma, H. Z. Chang, L. Chen, Y. Peng and N. Q. Yan, Appl. Catal. B-environ, 2012, 117, 73-80.
21. M. Machida, M. Uto, D. Kurogi and T. Kijima, J. Mater. Chem., 2001, 11, 900-904.
22. G. Busca, L. Lietti, G. Ramis and F. Berti, Appl. Catal. B-environ, 1998, 18, 1-36.
23. F. Eigenmann, M. Maciejewski and A. Baiker, Appl. Catal. B-environ, 2006, 62, 311-318.
24. L. A. Chen, J. H. Li and M. F. Ge, Environ. Sci. Technol., 2010, 44, 9590-9596.
25. M. Kantcheva, J. Catal., 2001, 204, 479-494.
26. L. Chmielarz, P. Kustrowski, A. Rafalska-Lasocha and R. Dziembaj, Appl. Catal. B-environ, 2005, 58, 235-244.
27. L. Gang, B. G. Anderson, J. van Grondelle and R. A. van Santen, Appl. Catal. B-environ, 2003, 40, 101-110.
28. S. J. Yang, C. X. Liu, H. Z. Chang, L. Ma, Z. Qu, N. Q. Yan, C. Z. Wang and J. H. Li, Ind. Eng. Chem. Res., 2013, 52, 5601-5610.
29. S. Yang, Y. Fu, Y. Liao, S. Xiong, Z. Qu, N. Yan and J. Li, Catal. Sci. Technol., 2014, 4, 224-232.